OPEN

Citation: Transl Psychiatry (2017) 7, e1009; doi:10.1038/tp.2016.283

www.nature.com/tp

ORIGINAL ARTICLE

White matter changes in microstructure associated with a maladaptive response to stress in rats

R Magalhães[1,2,3,9], J Bourgin[1,4,5,9], F Boumezbeur[6], P Marques[1,2,3], M Bottlaender[6], C Poupon[6], B Djemai[6], E Duchesnay[6], S Mériaux[6], N Sousa[2,3], TM Jay[1,4,5,10] and A Cachia[1,4,7,8,10]

In today's society, every individual is subjected to stressful stimuli with different intensities and duration. This exposure can be a key trigger in several mental illnesses greatly affecting one's quality of life. Yet not all subjects respond equally to the same stimulus and some are able to better adapt to them delaying the onset of its negative consequences. The neural specificities of this adaptation can be essential to understand the true dynamics of stress as well as to design new approaches to reduce its consequences. In the current work, we employed *ex vivo* high field diffusion magnetic resonance imaging (MRI) to uncover the differences in white matter properties in the entire brain between Fisher 344 (F344) and Sprague–Dawley (SD) rats, known to present different responses to stress, and to examine the effects of a 2-week repeated inescapable stress paradigm. We applied a tract-based spatial statistics (TBSS) analysis approach to a total of 25 animals. After exposure to stress, SD rats were found to have lower values of corticosterone when compared with F344 rats. Overall, stress was found to lead to an overall increase in fractional anisotropy (FA), on top of a reduction in mean and radial diffusivity (MD and RD) in several white matter bundles of the brain. No effect of strain on the white matter diffusion properties was observed. The strain-by-stress interaction revealed an effect on SD rats in MD, RD and axial diffusivity (AD), with lower diffusion metric levels on stressed animals. These effects were localized on the left side of the brain on the external capsule, corpus callosum, deep cerebral white matter, anterior commissure, endopiriform nucleus, dorsal hippocampus and amygdala fibers. The results possibly reveal an adaptation of the SD strain to the stressful stimuli through synaptic and structural plasticity processes, possibly reflecting learning processes.

Translational Psychiatry (2017) **7,** e1009; doi:10.1038/tp.2016.283; published online 24 January 2017

INTRODUCTION

Stress is a major risk factor to the development of severe mental illnesses, including major depression, anxiety,[1,2] bipolar disorders and schizophrenia (for review, see Walker *et al.*[3]) and overall one of the more common factors in eliciting dynamic changes in brain states.[4] Stress is known to trigger the activation of the hypothalamus–pituitary–adrenal axis, culminating in the production of glucocorticoids by the adrenals[5,6] that will in turn generate, depending on the individual and the stress stimulus characteristics, adaptive or maladaptive psychoneuroendocrine responses to the stressful stimulus.[7] In patients with major depressive disorder, dysregulation of the hypothalamus–pituitary–adrenal axis elicits specific and long-lasting functional and structural changes on a network of regions encompassing the hippocampus,[8–10] the medial prefrontal cortex[11,12] and amygdala.[13,14] Subjects with ultrahigh risk for psychosis are particularly sensitive to social stress, life events and daily hassles, which have the potential to trigger psychiatric symptoms; they have an increased basal cortisol level[15,16] and a smaller hippocampal volume.[17,18] Moreover, stressful life events in non-psychiatric subjects are associated with a gray matter volume decrease in a network encompassing the anterior cingulate cortex, the hippocampus and the parahippocampal gyrus that was observed within a 3-month period.[19]

Animal models have confirmed the drastic effects that stress can have on the brain, including changes in dendritic trees, synaptic plasticity inhibition in the hippocampus and the hippocampal-to-prefrontal pathway,[12,20,21] decreased neurogenesis in the hippocampus[22] and apoptosis, involving corticosteroids and glutamate receptors.[23] Taken together, these findings support the effect of stress on structural changes within networks of spatially distributed gray matter regions.

In addition to these regional changes, increasing evidence suggests that stress may also disrupt the structural and functional connectivity within neural networks.[24–28] Diffusion magnetic resonance imaging (dMRI) is an advanced technique for examining white matter (WM) anatomy providing insights on the pathway microstructure within neural networks.[29] A commonly used feature in dMRI studies is fractional anisotropy (FA), which estimates the degree to which tissue organization limits diffusion of water molecules in brain WM.[30] In animals, different recent dMRI studies investigated changes in diffusion signal associated to

[1]Physiopathologie des Maladies Psychiatriques, UMR_S 894 Inserm, Centre de Psychiatrie et Neurosciences, Paris, France; [2]Life and Health Sciences Research Institute (ICVS), School of Medicine, University of Minho, Campus de Gualtar, Braga, Portugal; [3]ICVS/3B's—PT Government Associate Laboratory, Braga/Guimarães, Portugal; [4]Université Paris Descartes, Sorbonne Paris Cité, Paris, France; [5]Faculté de Médecine Paris Descartes, Service Hospitalo Universitaire, Centre Hospitalier Sainte-Anne, Paris, France; [6]Neurospin, I2BM, CEA, Gif/Yvette, France; [7]Laboratoire de Psychologie du développement et de l'Education de l'Enfant, CNRS UMR 8240, Paris, France and [8]Institut Universitaire de France, Paris, France. Correspondence: Professor A Cachia, Centre de Psychiatrie et Neurosciences, INSERM UMR_S 894, 2 ter rue d'Alésia, Paris 75014, France.
E-mail: arnaud.cachia@parisdescartes.fr
[9]These authors share first author position.
[10]These authors share senior authorship.
Received 29 November 2016; accepted 30 November 2016

chronic stress exposure. Delgado y Palacios *et al.*[31] were the first to report the effects of stress using *in vivo* dMRI in rats: using diffusion kurtosis imaging (DKI), hippocampus microstructure was revealed to be altered in chronically stressed rats, independently of the hedonic state. More recently, the same team evaluated the mean kurtosis in the PFC, caudate–putamen (CPu) and amygdala in anhedonic-like and resilient rats and found a decrease in the CPu in the anhedonic-like.[32] In addition, using a similar chronic mild stress (CMS) model, Kumar *et al.*[33] showed increases in axial diffusion (AD) and radial diffusion (RD) specifically in the CPu and the amygdala of stressed rats. Another study using *in vivo* dMRI showed an increase in the mean diffusion (MD) in the lateral ventricles of chronically stressed rats, although no other changes were found.[27] Finally, using a mice and a social defeat stress paradigm, Anacker *et al.*[28] have shown correlations between diffusion metrics and social avoidance correlating positively with FA in the hypothalamus and hippocampus.

Here, we used dMRI and the tract-based spatial statistics (TBSS) approach[34] adapted to brain rat to investigate the WM microstructure on the entire brain. We selected two strains of rats, Fischer 344 (F344) and Sprague–Dawley (SD), known to have differential response to stress,[35,36] and compared their WM microstructure, assessed by four complementary dMRI measures (FA, MD, AD and RD), after exposure to repeated inescapable stress. Repeated exposure to the same stressor very often results in habituation, which leads to a decrease in the hypothalamus–pituitary–adrenal axis response.[37] In contrast to SD rats, F344 rats show virtually no habituation or adaptation of the corticosterone stress response during repeated stress but an exaggerated acute stress-induced corticosterone secretion[35,36] and increased anxiety-related behaviors[38] with increased amygdala volume.[39] Such a design allowed studying the effect, but also the responsivity, to stress.

MATERIALS AND METHODS

Animals

Experiments were performed with male adult SD ($n = 14$) and Fisher 344 (F344; $n = 14$) rats (Charles River, Saint-Germain-sur-l'Arbresle, France) at 8 weeks' age (average of 200 g for SD and 180 g for F344). Rats were housed in groups of two animals with *ad libitum* access to food and water and maintained in a temperature-controlled room, with a light/dark cycle of 12/12 h (lights on at 0600 hours). For each strain, rats were randomly assigned to stressed ($N = 14$) and non-stressed ($N = 14$) groups. Two animals of the SD strain of the control group were killed before the end of the 2 weeks. The protocols have been approved by the *Comité d´ Éthique en Expérimentation Animale du Commissariat à l´ Énergie Atomique et aux Energies Alternatives—Direction des Sciences du Vivant Ile de France* (CETEA/CEA/DSV IdF) under protocol ID 12-058. All procedures were conducted in conformity with National (JO 887–848) and European (86/609/EEC) rules for animal experimentation.

Stress protocol

The behavioral stress protocol has been previously described elsewhere.[20] Briefly, rats were placed on an elevated and unsteady platform for 30 min. The platform was positioned 1 m above the ground and illuminated with a high-intensity light source (1500 Lux). While on the platform, animals showed urination, defecation, grooming and freezing. This inescapable stress exposure (called a session) was repeated daily during 15 days between 0900 and 1200 hours.[40] We measured corticosterone levels for all animals in control condition and after the end of the stress session. Animals were randomly chosen to be stressed or not. This protocol was chosen as we previously demonstrated that it causes with a similar sample size a disruption of synaptic plasticity in the hippocampal-to-prefrontal cortex pathway[20] and changes in regional brain volumes that are associated with an increase in plasma corticosterone levels.[39]

Corticosterone immunoassay

The plasma level of corticosterone was assessed as a biomarker of stress in all experiments. Blood samples were collected from the tail under quick anesthesia in basal conditions on day 0 (D0) and 10 min after the end of the stress session at different times (acute stress: D1; repeated stress: D15) for the group exposed to stress. Blood samples for the control group were taken at D15. Anesthesia was induced with 5% isoflurane mixed with oxygen, using a calibrated vaporizer maintained at 2% during the sampling. Samples were centrifuged at 1000 *g* for 15 min, and serum stored at − 20 °C. Plasma corticosterone was assessed by immunoassay (Corticosterone Immunoassay, Enzo Life Sciences, Villeurbane, France).

Tissue preparation

Twenty-four hours after the last day of repeated inescapable stress or after daily handling in control animals, rats were anesthetized with sodium pentobarbital (100–150 mg kg^{-1}, intraperitoneally (i.p.)), followed by intracardiac perfusion with physiological NaCl solution and 4% cold paraformaldehyde in 0.01 M phosphate-buffered saline (pH = 7.4). After perfusion, the brain was harvested maintaining integrity and stored in 4% PFA in phosphate-buffered saline at 4 °C. Before MRI, the brains were washed into phosphate-buffered saline for 24 h to remove the fixation solution and then placed into a custom-built MRI-compatible tube. The tube was filled with Fluorinert, an MRI susceptibility-matching fluid (Sigma-Aldrich, St Louis, MO, USA).

Acquisition of diffusion MRI data

Diffusion *ex vivo* data with high spatial and angular resolution were acquired to quantify the subtle changes in the WM microstructure within the entire rat brain. The *ex vivo* MRI acquisitions were performed on a 7 T preclinical scanner (PharmaScan, Bruker, Ettlingen, Germany) using a home-made quadrature birdcage coil (inside diameter = 28 mm). Diffusion images were acquired using a Spin-Echo Multi Shot Echo Planar Imaging (repetition time (TR) = 26 s, echo time (TE) = 29 ms, 90° excitation pulse followed by a 180° refocusing pulse, 4 segments, 4 averages, total time = 24 h16 m 03 s). One hundred four interleaved slices with 0.25 mm thickness were acquired, with a matrix size of 106 × 106, a field-of-view of 25.44 × 25.44 mm and an in-plane resolution of 0.24 × 0.24 mm. Following 10 acquisitions with no diffusion sensitization ($b = 0$ s mm^{-2}), diffusion-weighted images were acquired along 200 noncollinear directions ($b = 4000$ s mm^{-2}). The physicist performing the MRI acquisition was blind to the group allocation (stress versus no stress).

Preprocessing of diffusion MRI

The dMRI images were reconstructed using an in-house script and visually inspected for brain lesions and artefacts, after which two subjects (one F344 and one SD from the control group) were excluded because of the presence of artefacts. All the data were pre-processed using the FMRIB Software Library[41] (FSL, http://fsl.fmrib.ox.ac.uk/fsl/) v5.0.6 using the following steps: bias field correction using FAST,[42] correction of the field inhomogeneity, estimated from b0 images, on all volumes; eddy current distortions and movement correction with fsl 'eddy_correct' command-line tool (the first volume without diffusion sensitization was chosen as the reference volume for the affine registration); segmentation of the brain signal using BET:[43] BET was applied to the mean of the images without diffusion sensitization, with the resulting mask being applied to all volumes. The gradient vector directions were rotated for each subject according to the eddy correct output.[44]

Tensor fitting and scalar maps were calculated using FSL FDT 'dtifit' command line[45,46] using the corrected vector directions. These maps were used to obtain the FA, AD, MD and RD maps (see Figure 1). These indexes derived from dMRI provide complementary information of WM microstructure. Although discussed, FA is classically considered to reflect the degree of myelination and axonal density.[47–50] AD measures diffusivity parallel to axonal fibers and AD decreases are thought to reflect pathology of the axon itself, such as from trauma or ischemic changes.[47] RD measures diffusivity perpendicular to axonal fibers and appears to be more strongly correlated with myelin abnormalities, like demyelination, as observed in multiple sclerosis.[51]

TBSS

Whole-brain voxel-based statistical analysis was performed using the TBSS approach[34] distributed as part of FSL adapted to the rat brain. The FA maps

of all subjects obtained in the tensor-fitting step were aligned into a common space using a study-dedicated template and the nonlinear registration tool FNIRT.[52] The template was defined as the most representative animal, calculated during the TBSS pipeline as the one that minimizes transformations. Next, all the FA images were averaged and thinned in order to create the mean FA skeleton. A threshold of 0.3 was applied to this skeleton in order to restrict the analysis to the WM tracts, and thus defining the final voxels for analysis. The AD, MD and RD maps of all animals were then warped into this skeleton map using the nonlinear transformations previously calculated for the FA maps.

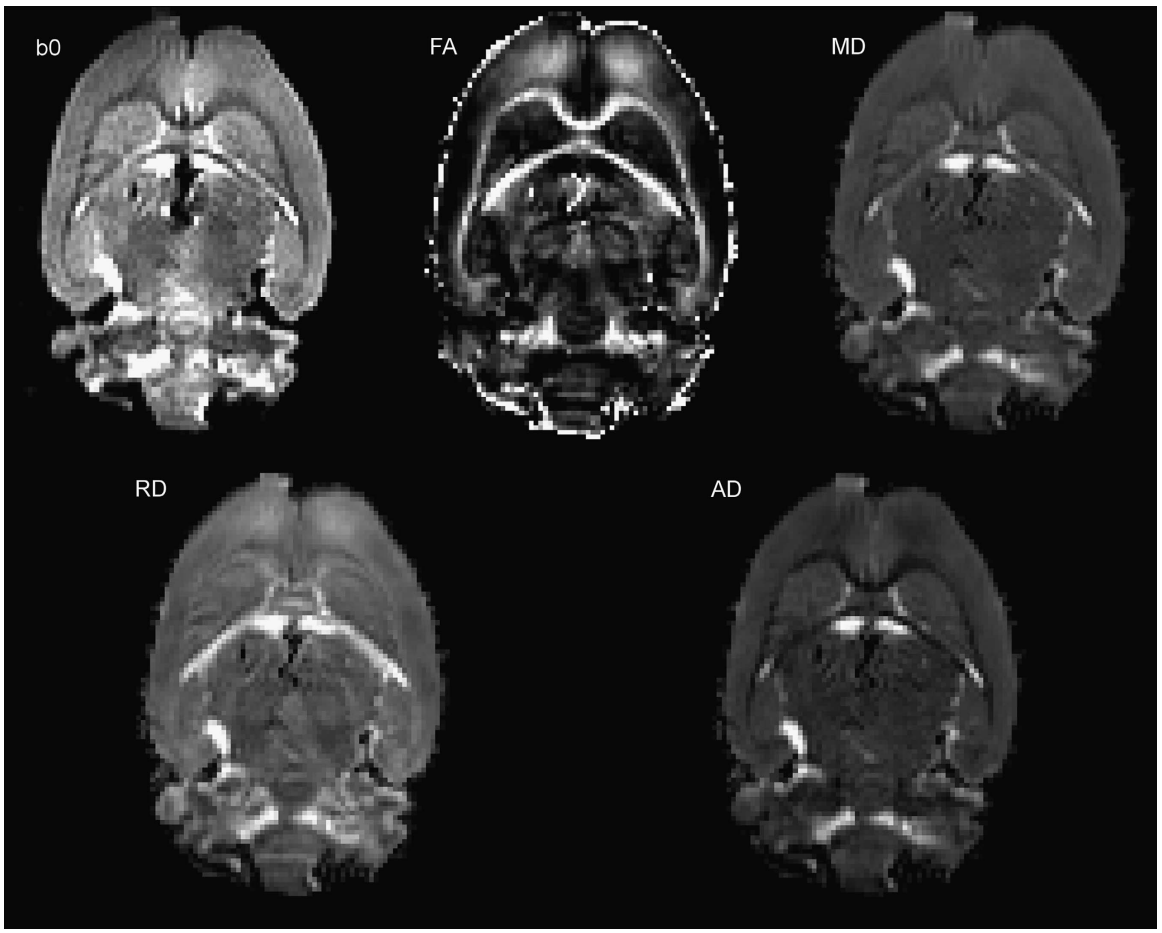

Figure 1. Representative image of the diffusion MRI data (b0 map) and diffusion metrics (FA, MD, RD, AD) in a rat brain**.** AD, axial diffusivity; FA, fractional anisotropy; MD, mean diffusivity; MRI, magnetic resonance imaging; RD, radial diffusivity**.**

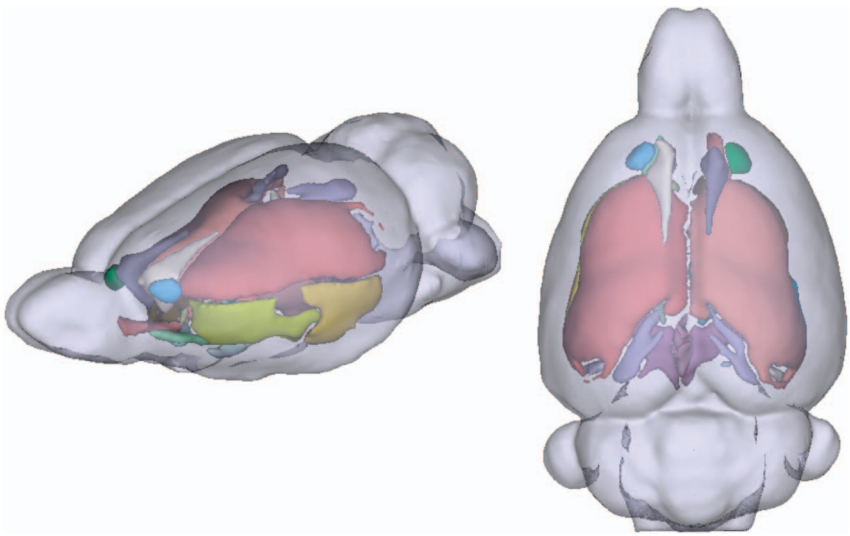

Figure 2. Three-dimensional reconstructions of the white matter skeleton used for TBSS analyses (lateral and top views). White matter tracts were color-coded based on the Paxinos and Watson atlas.[54] TBSS, tract-based spatial statistics**.**

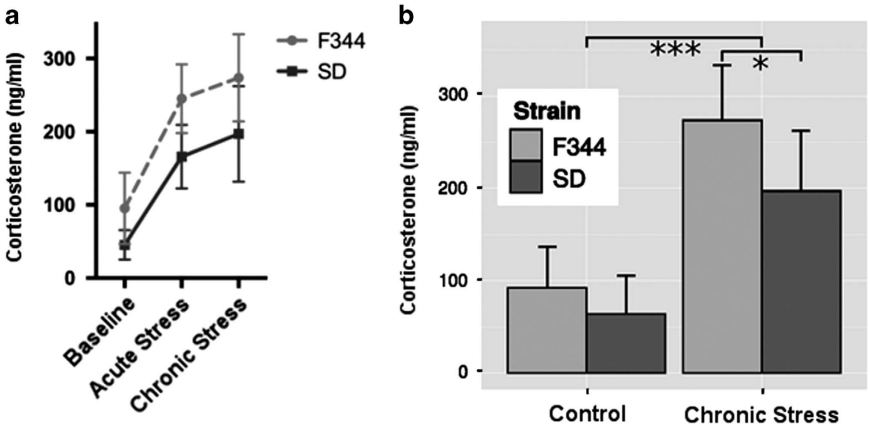

Figure 3. Plasma levels of corticosterone (mean ± s.d.) obtained in control and after stress in F344 and SD rats. (**a**) Longitudinal data at baseline (D0), after acute stress (D1) and after chronic stress (D15). (**b**) Comparison between strains before stress (D0) and after chronic stress (D15). Significance levels: $*P < 0.05$, $***P < 0.001$. F344, Fischer 344; SD, Sprague–Dawley.

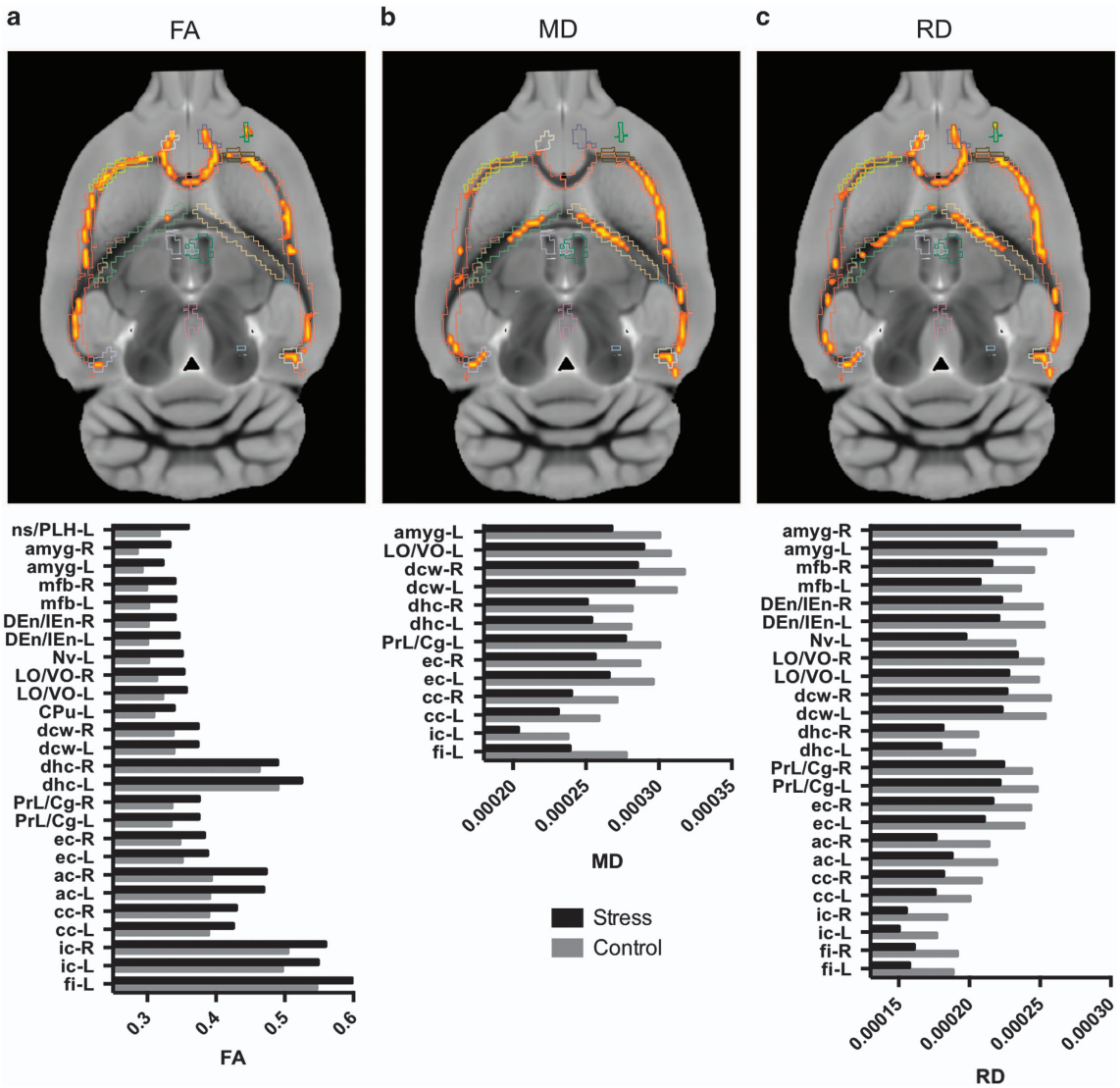

Figure 4. White matter tracts with microstructural differences between control rats and stressed rats. Top panel represents an axial brain slice with voxels with significant main effect of stress (red–yellow scale) superimposed on the white matter skeleton used for TBSS analyses. Bottom panel provides histogram of white matter tracts microstructure (FA, MD or RD) in control (black) and stressed (light gray) rats. Only tracts with significant main effect of stress on FA (**a**), MD (**b**) or RD (**c**) are represented. For illustration purpose, the tracts were slightly dilated. FA, fractional anisotropy; MD, mean diffusivity; RD, radial diffusivity; TBSS, tract-based spatial statistics.

Statistical analysis for the skeletonized maps of FA, AD, MD and RD was performed using the 'randomise' fsl command-line tool, yielding a non-parametric test based on randomization methods. A total of 10 000 random permutations were used with threshold-free cluster enhancement,[53] and multiple comparison corrections for family-wise error results were considered significant at $P < 0.05$. Six different contrasts were calculated, testing for the effect of stress ('Stress > No stress'; 'Stress < No stress'), strain ('SD > F344'; 'SD < F344') and stress-by-strain interaction.

Labeling of significant clusters in the FA skeleton was based on the standard Paxinos and Watson atlas[54] and cross-validated by visual inspection (Figure 2). Descriptive statistics were then calculated separately for each WM bundles.

RESULTS

Corticosterone plasma level

As expected, we found a significant main effect of stress on corticosterone plasma levels ($F(25, 1) = 54.87$, $P = 2.7 \times 10^{-7}$) after chronic stress exposure (increase) in both strains ((SD rats: $n = 6$, 197 ± 65.34 ng ml^{-1} and F344 rats: $n = 8$, 273.75 ± 59.50 ng ml^{-1}) when compared with non-stressed rats (SD rats: $n = 6$, 63.66 ± 41.86 ng ml^{-1} and F344 rats: $n = 6$, 92.50 ± 44.01 ng ml^{-1}). There was also a significant difference between the two strains after 15 days of stress exposure with a higher plasma corticosterone level in F344 rats compared with SD rats ($T(11) = 2.18$, $P = 0.02$; Figure 3). There was no variance difference in corticosterone plasma levels between strains (SD versus F344) in control and stressed animals nor difference between conditions (stress versus no stress) in SD and F344 (Fligner–Killeen non-parametric test of homogeneity of variances, all P-values > 0.2).

White matter microstructure

The final number of animals involved in the analysis was as follows: 11 SD rats (four control and seven stressed) and 13 F344 (six control and seven stressed).

The WM skeleton in which statistical tests were conducted was constituted by a total of 6254 voxels. All the statistical tests were done with 23 degrees of freedom.

TBSS analyses revealed no significant main effect of strain ('F344' versus 'SD') in FA, AD, MD or RD maps ($P_{corrected} > 0.05$).

In contrast, we found a main effect of stress ('control' versus 'stress') in several WM bundles, with increased FA (peak T-value = 5.720, peak-corrected P-value = 0.012, cluster size of 3126 voxels) and decreased RD (peak T-value = 4.621, peak-corrected P-value = 0.011, cluster size of 3480 voxels) and MD (peak T-value = 4.598, peak-corrected P-value = 0.037, cluster size of 1515 voxels) in stressed animals compared with controls (Figure 4). These stress-related differences were distributed over the entire brain and involved WM bundles in posterior and anterior areas, on both hemispheres (Table 1).

Finally, significant strain-by-stress interactions were found in MD, RD and AD maps (Figure 5), with a stress-related decrease in SD rats and an absence of change in F344 rats. Significant interactions involved WM bundles in the left hemisphere and included the following: the corpus callosum (cc), external capsule (ec) and deep cerebral WM (dcw) for MD, RD and AD measures; the anterior commissure (ac), dorsal and intermediate endopiriform nucleus (DEn/IEn) and amygdala for MD and RD measures; and dorsal hippocampus commissure (dhc) on MD. All statistics related to these results can be found on Table 2.

Table 1. Abbreviations of the white matter tracts investigated in the study

Abbreviation	*White matter tract*
ac	Anterior commissure
amygfib	Amygdala fibers
cc	Corpus callosum
dcw	Deep cerebral white matter
denien	Dorsal and intermediate endopiriform nucleus fibers
dhc	Dorsal hippocampus commissure
ec	External capsule
fi	Fimbria of the hippocampus
ic	Internal capsule
inwh	Intermediate white layer
lovo	Lateral orbital cortex/ventral orbital cortex
mfb	Medial forebrain bundle
nsplh	Nigrostriatal bundle/peduncular part of the lateral hypothalamus
nv	Navicular nu basal forebrain
opt	Optic tract
optot	Olivary pretectal nu/nu of the optic tract
prlcg	Prelimbic cortex/cingulate cortex
strfibers	Striatum fibers
strmlfr	Superior thalamic radiation/medial lemniscus/ fasciculus retroflexus

White matter tracts were labeled based on the Paxinos and Watson atlas.[54]

DISCUSSION

This diffusion MRI study reveals that 15 days of repeated exposure to the same inescapable stressor in rats leads to microstructural WM changes—increased FA and decreased MD and RD—of several WM bundles distributed in the entire brain. Furthermore, differential stress effects were observed in SD and F344 rat strains, which are known to have a different behavioral and physiological habituation to repeated stress.[35,36]

Several WM bundles reported in this study (including amygdala fibers, dcw, DEn/IEn fibers, dorsal hippocampus, fimbria of the hippocampus, external capsule and corpus callosum) connect brain areas associated with emotion formation and processing, attention, and learning and memory.[14,55–57] Of note, some of these bundles interconnect the hippocampus (dhc and fi) or connect the hippocampus to the amygdala, prefrontal cortex and anterior thalamic nuclei (ec, cc, StrlCg and dcw), regions consistently reported to be affected by stress.[7,9,10,12,14] Changes found in ac, proximal to the olfactory bulb and in Denien[58] may indicate a stress-related alteration in sensory circuits, possibly because of a readjustment of the perception of their surroundings.

To our knowledge, this is the first study to show the effects of repeated acute stress exposure in two strains with different stress sensitivity and habituation. Indeed, we show decreased MD, RD and AD in several brain bundles in SD rats, whereas no such differences were observed in F344 rats. This is particularly relevant, as SD rats were able to adjust their stress response to the repeated exposure to acute stress (resilience), therefore, showing an adaptive response that may be triggered by the acquisition of coping mechanisms that are paralleled by the decreases in MD, RD and AD, despite the overall increase in FA. In contrast, F344 (nonresilient) rats, which display a maladaptive response, do not reveal significant changes in these parameters. These findings suggest that differential response to repeated acute stressors may be revealed by or are associated with the ability to trigger structural plastic events in WM.

A few preclinical dMRI studies previously reported measurable effects of stress on several brain regions, and in all cases addressing the impact of chronic stress. Indeed, a significant decrease in the mean and radial kurtosis in the hippocampus was detected following CMS in rats.[31] More recently, the same team reported significant stress-related increases in AD and RD in the CPu and in the amygdala, respectively, along with a mean kurtosis decrease in the CPu in anhedonic-like animals compared with resilient animals.[32] Such effects were interpreted as the result of

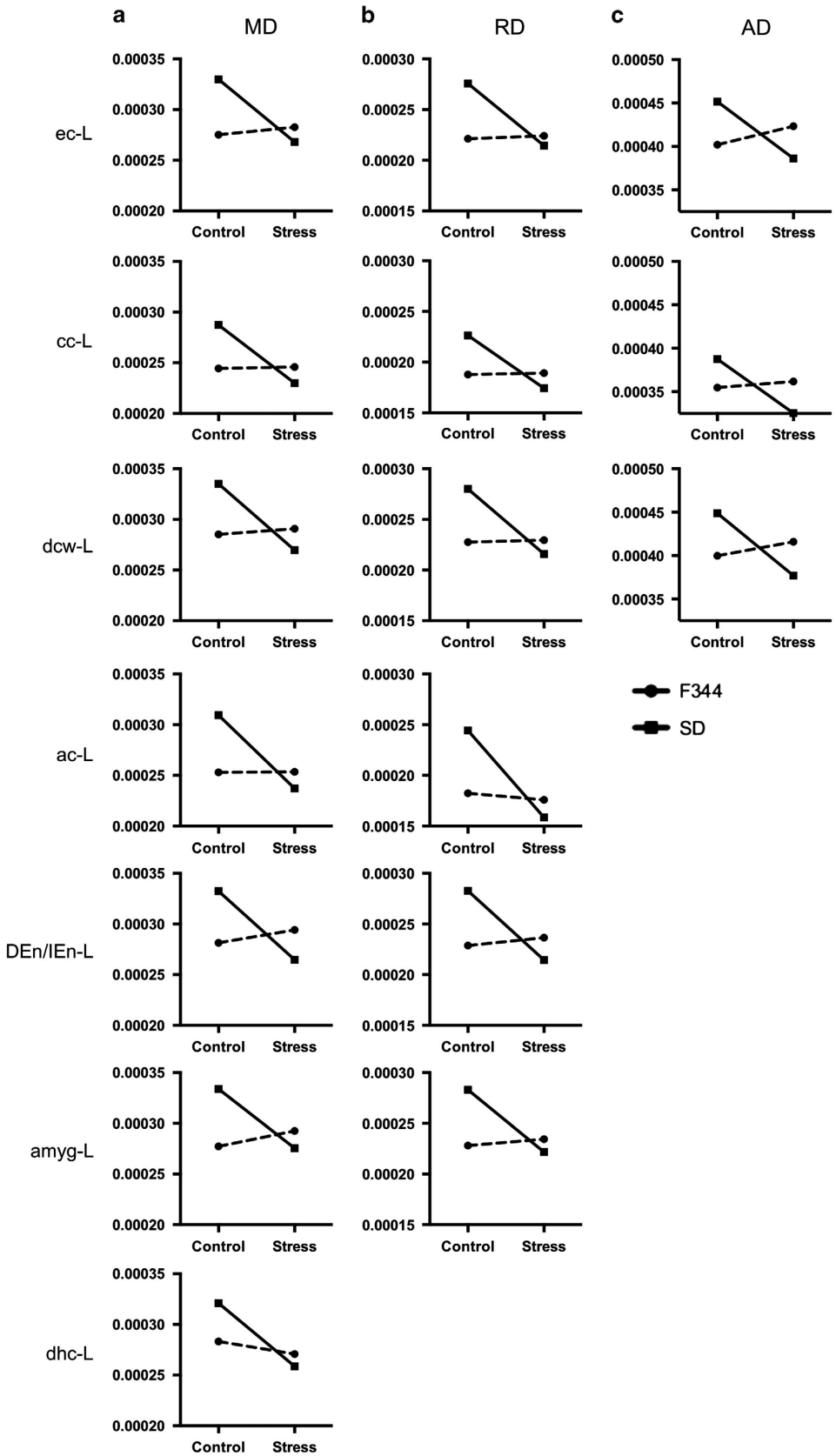

Figure 5. White matter tract changes in microstructure associated with maladaptative response to stress. Interaction graphs provide the mean values of white matter tract microstructure - FA (**a**), MD (**b**) or RD (**c**) - in control (black) and stressed (light gray) animals, in F344 (circles with solid lines) and SD (squares with dotted lines) rats. ac, anterior commissure; amygFib, amygdala fiber; cc, corpus callosum; dcw, deep cerebral white matter; denien, dorsal and intermediate endopiriform nucleus fiber; dhc, dorsal hippocampus commisure; ec, external capsule; FA, fractional anisotropy; F344, Fischer 344; MD, mean diffusivity; RD, radial diffusivity; SD, Sprague–Dawley.

Table 2. Statistics of the white matter tracts associated with maladaptive response to stress

White matter tract	*MD*	*RD*	*AD*
External capsule (ec)			
Peak *T*-value	3.62	3.55	3.35
Peak *P*-value	0.041	0.048	0.043
# Voxels	219	26	205
Corpus callosum (cc)			
Peak *T*-value	4.17	3.66	3.65
Peak *P*-value	0.041	0.035	0.049
# Voxels	104	114	15
Deep cerebral white matter (dcw)			
Peak *T*-value	3.89	3.264	4.39
Peak *P*-value	0.041	0.043	0.048
# Voxels	199	154	117
Anterior commissure (ac)			
Peak *T*-value	4.05	4.41	—
Peak *P*-value	0.043	0.044	—
# Voxels	23	23	—
Dorsal and intermediate endopiriform nucleus fibers (denien)			
Peak *T*-value	2.97	2.69	—
Peak *P*-value	0.046	0.048	—
# Voxels	8	7	—
Amygdala fibers (amyg)			
Peak *T*-value	2.56	2.50	—
Peak *P*-value	0.042	0.045	—
# Voxels	1	2	—
Dorsal hippocampus commissure (dhc)			
Peak *T*-value	2.72	—	—
Peak *P*-value	0.049	—	—
# Voxels	2	—	—

Abbreviations: AD, axial diffusivity; MD, mean diffusivity; RD, radial diffusivity. The peak *T*-value, the corresponding peak *P*-value and the number of voxels in the cluster are provided for white matter tracts with significant strain-by-stress interactions on MD, RD and AD.

axonal degeneration and demyelination within WM bundles with disrupted microstructural spatial coherence. A FA decrease interpreted as a potential loss of myelin sheath was also found in the corpus callosum, bilateral frontal cortex and bilateral hypothalamus in rats after a similar CMS protocol.[33]

Such contrasting results are likely to reflect the temporal dynamics of the stress response (and its successful, or not, adaptation). Yet, we cannot exclude that other methodological differences may also explain the difference in FA change direction, including the stress paradigm (repeated acute stress versus CMS), image acquisition (*in vivo* dMRI versus *ex vivo* data with higher spatial resolution and higher signal-to-noise ratio) or image analysis (measure in *a priori* preselected regions of interest, mostly within gray matter structures versus voxel-wise analysis on the whole WM tracts).

Increased WM FA has been repeatedly associated to learning[59–61] via neuronal plasticity processes (for example, synaptogenesis and dendritic branching) and glial remodeling (for example, modification of astrocyte processes).[62] An increased FA was found in the corpus callosum after a spatial learning task and such increase was supported by significant increases in immune reactivity for a myelin marker, suggesting an increase in the cellular organization and packing of axons or myelin.[59,63] More recently, TBSS analysis also revealed higher FA in skilled learning rats in comparison with control[64] that could be explained by increases in myelination. On the other hand, a reduction in MD was found in both rat hippocampi before and after learning a hippocampal-dependent spatial navigation task.[61] Data from both human and animal studies indicate the potential for rapid changes in dMRI indices,[61,65] suggesting changes in structural plasticity in specific brain regions. The patterns of FA increase/RD decrease are likely related to a tissue density increase due to reshaping of neuronal or glial processes, and/or enhancement of tissue organization, including strengthening of axonal or dendritic backbones and surrounding tissue.[66] Myelination, known to be modified by experience and maturation,[67,68] may also partly explain the RD decrease observed in the stressed rats as RD increases have previously been associated with demyelination processes.[69,70] Of note, an activity-dependent myelination has been recently proposed in a human study of motor training, where the FA change in WM was accompanied by adjacent gray matter density alterations.[71]

This study presents some limitations that should be considered. Here the susceptible/resilient differences are achieved by using different strains. We cannot discard the possibility that the mechanisms that lead to different responses to stress within a single strain are different, or if the results found are specific to the SD strain, making its generalization harder. In addition, corticosterone was the only measure used to access the stress response, and although it is known to be one of the more representative markers of stress, the use of complementary behavioral assessment could be beneficial. Other limitations include the lack of direct histological correlations between DTI indices and morphological markers due to the exclusive *ex vivo* approach. *In vivo* longitudinal measurements would have allowed comparisons before and after stress, however, at the expense of signal-to-noise ratio and diffusion MRI spatial and angular resolution.

To conclude, we identified microstructural changes in the key WM tracts like the corpus callosum and the amygdala fibers linked to the frontolimbic circuitry with a functional relevance for cognitive performance and emotional response. Our data demonstrate that SD rats able to adjust to repeated exposure to an acute stress leads to significant changes in dMRI indices. These changes are not well understood, but we demonstrate that dMRI may offer a novel measure of microstructural remodeling occurring in response to stress to further explore the neural basis of adaptive and maladaptive response to stress in rodents and provide quantitative biomarkers to evaluate novel treatments to the protection of stress effects.

CONFLICT OF INTEREST

The authors declare no conflict of interest.

ACKNOWLEDGMENTS

We thank Neurospin (high field MRI center CEA Saclay) for providing its support for MRI acquisition. JB was supported by grants from Fondation pour la Recherche Médicale (FRM) and Groupe Pasteur Mutualité (GPM). This work was supported by a grant from ANR (SIGMA). This work was performed on a platform of France Life Imaging (FLI) network partly funded by the grant ANR-11-INBS-0006. This work and RM were supported by a fellowship of the project FCT-ANR/NEU-OSD/0258/2012 founded by FCT/MEC (www.fct.pt) and by Fundo Europeu de Desenvolvimento Regional (FEDER). AC was supported by a grant from the Fondation NRJ.

REFERENCES

1 Kendler KS, Karkowski LM, Prescott CA. Causal relationship between stressful life events and the onset of major depression. *Am J Psychiatry* 1999; **156**: 837–841.
2 Grillon C, Lissek S, Rabin S, McDowell D, Dvir S, Pine DS. Increased anxiety during anticipation of unpredictable but not predictable aversive stimuli as a psychophysiologic marker of panic disorder. *Am J Psychiatry* 2008; **165**: 898–904.

3 Walker E, Mittal V, Tessner K. Stress and the hypothalamic pituitary adrenal axis in the developmental course of schizophrenia. *Annu Rev Clin Psychol* 2008; **4**: 189–216.
4 Sousa N. The dynamics of the stress neuromatrix. *Mol Psychiatry* 2016; **21**: 302–312.
5 Whitnall MH. Regulation of the hypothalamic corticotropin-releasing hormone neurosecretory system. *Prog Neurobiol* 1993; **40**: 573–629.
6 Jacobson L. Hypothalamic-pituitary-adrenocortical axis regulation. *Endocrinol Metab Clin N Am* 2005; **34**: 271–292, vii.
7 McEwen BS. The neurobiology of stress: from serendipity to clinical relevance. *Brain Res* 2000; **886**: 172–189.
8 Sheline YI, Mittler BL, Mintun MA. The hippocampus and depression. *Eur Psychiatry* 2002; **17**: 300–305.
9 McEwen BS. Mood disorders and allostatic load. *Biol Psychiatry* 2003; **54**: 200–207.
10 Sousa N, Lukoyanov NV, Madeira MD, Almeida OF, Paula-Barbosa MM. Erratum to 'Reorganization of the morphology of hippocampal neurites and synapses after stress-induced damage correlates with behavioral improvement'. *Neuroscience* 2000; **101**: 483.
11 Mayberg HS, Lozano AM, Voon V, McNeely HE, Seminowicz D, Hamani C *et al.* Deep brain stimulation for treatment-resistant depression. *Neuron* 2005; **45**: 651–660.
12 Cerqueira JJ, Mailliet F, Almeida OFX, Jay TM, Sousa N. The prefrontal cortex as a key target of the maladaptive response to stress. *J Neurosci* 2007; **27**: 2781–2787.
13 Pruessner JC, Dedovic K, Pruessner M, Lord C, Buss C, Collins L *et al.* Stress regulation in the central nervous system: evidence from structural and functional neuroimaging studies in human populations—2008 Curt Richter Award Winner. *Psychoneuroendocrinology* 2010; **35**: 179–191.
14 Roozendaal B, McEwen BS, Chattarji S. Stress, memory and the amygdala. *Nat Rev Neurosci* 2009; **10**: 423–433.
15 Tessner KD, Mittal V, Walker EF. Longitudinal study of stressful life events and daily stressors among adolescents at high risk for psychotic disorders. *Schizophr Bull* 2011; **37**: 432–441.
16 Chaumette B, Kebir O, Mam-Lam-Fook C, Morvan Y, Bourgin J, Godsil BP *et al.* Salivary cortisol in early psychosis: new findings and meta-analysis. *Psychoneuroendocrinology* 2016; **63**: 262–270.
17 Aiello G, Horowitz M, Hepgul N, Pariante CM, Mondelli V. Stress abnormalities in individuals at risk for psychosis: a review of studies in subjects with familial risk or with 'at risk' mental state. *Psychoneuroendocrinology* 2012; **37**: 1600–1613.
18 Collip D, Habets P, Marcelis M, Gronenschild E, Lataster T, Lardinois M *et al.* Hippocampal volume as marker of daily life stress sensitivity in psychosis. *Psychol Med* 2013; **43**: 1377–1387.
19 Papagni SA, Benetti S, Arulanantham S, McCrory E, McGuire P, Mechelli A. Effects of stressful life events on human brain structure: a longitudinal voxel-based morphometry study. *Stress* 2010; **14**: 227–232.
20 Rocher C, Spedding M, Munoz C, Jay TM. Acute stress-induced changes in hippocampal/prefrontal circuits in rats: effects of antidepressants. *Cereb Cortex* 2004; **14**: 224–229.
21 Shakesby AC, Anwyl R, Rowan MJ. Overcoming the Effects of stress on synaptic plasticity in the intact hippocampus: rapid actions of serotonergic and antidepressant agents. *J Neurosci* 2002; **22**: 3638–3644.
22 Gould E, Tanapat P, McEwen BS, Flügge G, Fuchs E. Proliferation of granule cell precursors in the dentate gyrus of adult monkeys is diminished by stress. *Proc Natl Acad Sci USA* 1998; **95**: 3168–3171.
23 McEwen BS. Stress and hippocampal plasticity. *Annu Rev Neurosci* 1999; **22**: 105–122.
24 Sousa N, Almeida OF. Disconnection and reconnection: the morphological basis of (mal)adaptation to stress. *Trends Neurosci* 2012; **35**: 742–751.
25 Soares JM, Sampaio A, Ferreira LM, Santos NC, Marques F, Palha JA *et al.* Stress-induced changes in human decision-making are reversible. *Transl Psychiatry* 2012; **2**: e131.
26 Soares JM, Sampaio A, Ferreira LM, Santos NC, Marques P, Marques F *et al.* Stress impact on resting state brain networks. *PLoS One* 2013; **8**: e66500.
27 Henckens MJ, van der Marel K, van der Toorn A, Pillai AG, Fernandez G, Dijkhuizen RM *et al.* Stress-induced alterations in large-scale functional networks of the rodent brain. *NeuroImage* 2015; **105**: 312–322.
28 Anacker C, Scholz J, O'Donnell KJ, Allemang-Grand R, Diorio J, Bagot RC *et al.* Neuroanatomic differences associated with stress susceptibility and resilience. *Biol Psychiatry* 2015; **79**: 840–849.
29 Soares JM, Marques P, Alves V, Sousa N. A hitchhiker's guide to diffusion tensor imaging. *Front Neurosci* 2013; **7**: 31.
30 Basser PJ, Pierpaoli C. Microstructural and physiological features of tissues elucidated by quantitative-diffusion-tensor MRI. *J Magn Reson B* 1996; **111**: 209–219.
31 Delgado y Palacios R, Campo A, Henningsen K, Verhoye M, Poot D, Dijkstra J *et al.* Magnetic resonance imaging and spectroscopy reveal differential hippocampal changes in anhedonic and resilient subtypes of the chronic mild stress rat model. *Biol Psychiatry* 2011; **70**: 449–457.
32 Delgado y Palacios R, Verhoye M, Henningsen K, Wiborg O, Van der Linden A. Diffusion kurtosis imaging and high-resolution MRI demonstrate structural aberrations of caudate putamen and amygdala after chronic mild stress. *PLoS One* 2014; **9**: e95077.
33 Hemanth Kumar BS, Mishra SK, Trivedi R, Singh S, Rana P, Khushu S. Demyelinating evidences in CMS rat model of depression: A DTI study at 7T. *Neuroscience* 2014; **275C**: 12–21.
34 Smith SM, Jenkinson M, Johansen-Berg H, Rueckert D, Nichols TE, Mackay CE *et al.* Tract-based spatial statistics: voxelwise analysis of multi-subject diffusion data. *Neuroimage* 2006; **31**: 1487–1505.
35 Dhabhar FS, McEwen BS, Spencer RL. Adaptation to prolonged or repeated stress--comparison between rat strains showing intrinsic differences in reactivity to acute stress. *Neuroendocrinology* 1997; **65**: 360–368.
36 Dhabhar FS, Miller AH, McEwen BS, Spencer RL. Differential activation of adrenal steroid receptors in neural and immune tissues of Sprague Dawley, Fischer 344, and Lewis rats. *J Neuroimmunol* 1995; **56**: 77–90.
37 Natelson BH, Ottenweller JE, Cook JA, Pitman D, McCarty R, Tapp WN. Effect of stressor intensity on habituation of the adrenocortical stress response. *Physiol Behav* 1988; **43**: 41–46.
38 Uchida S, Nishida A, Hara K, Kamemoto T, Suetsugi M, Fujimoto M *et al.* Characterization of the vulnerability to repeated stress in Fischer 344 rats: possible involvement of microRNA-mediated down-regulation of the glucocorticoid receptor. *Eur J Neurosci* 2008; **27**: 2250–2261.
39 Bourgin J, Cachia A, Boumezbeur F, Djemaï B, Bottlaender M, Duchesnay E *et al.* Hyper-responsivity to stress in rats is associated with a large increase in amygdala volume. A 7T MRI study. *Eur Neuropsychopharmacol* 2015; **25**: 828–835.
40 Storey JD, Robertson DAF, Beattie JE, Reid IC, Mitchell SN, Balfour DJK. Behavioural and neurochemical responses evoked by repeated exposure to an elevated open platform. *Behav Brain Res* 2006; **166**: 220–229.
41 Smith SM, Jenkinson M, Woolrich MW, Beckmann CF, Behrens TE, Johansen-Berg H *et al.* Advances in functional and structural MR image analysis and implementation as FSL. *Neuroimage* 2004; **23**: S208–S219.
42 Zhang Y, Brady M, Smith S. Segmentation of brain MR images through a hidden Markov random field model and the expectation-maximization algorithm. *IEEE Trans Med Imaging* 2001; **20**: 45–57.
43 Smith SM. Fast robust automated brain extraction. *Hum Brain Mapp* 2002; **17**: 143–155.
44 Leemans A, Jones DK. The B-matrix must be rotated when correcting for subject motion in DTI data. *Magn Reson Med* 2009; **61**: 1336–1349.
45 Behrens TE, Berg HJ, Jbabdi S, Rushworth MF, Woolrich MW. Probabilistic diffusion tractography with multiple fibre orientations: what can we gain? *NeuroImage* 2007; **34**: 144–155.
46 Behrens TE, Woolrich MW, Jenkinson M, Johansen-Berg H, Nunes RG, Clare S *et al.* Characterization and propagation of uncertainty in diffusion-weighted MR imaging. *Magn Reson Med* 2003; **50**: 1077–1088.
47 Song S-K, Sun S-W, Ju W-K, Lin S-J, Cross AH, Neufeld AH. Diffusion tensor imaging detects and differentiates axon and myelin degeneration in mouse optic nerve after retinal ischemia.. *NeuroImage* 2003; **20**: 1714–1722.
48 Song S-K, Sun S-W, Ramsbottom MJ, Chang C, Russell J, Cross AH. Dysmyelination revealed through MRI as increased radial (but unchanged axial) diffusion of water. *NeuroImage* 2002; **17**: 1429–1436.
49 Arfanakis K, Haughton VM, Carew JD, Rogers BP, Dempsey RJ, Meyerand ME. Diffusion tensor MR imaging in diffuse axonal injury. *Am J Neuroradiol* 2002; **23**: 794–802.
50 Harsan LA, Poulet P, Guignard B, Steibel J, Parizel N, Loureiro de Sousa P *et al.* Brain dysmyelination and recovery assessment by noninvasive *in vivo* diffusion tensor magnetic resonance imaging. *J Neurosci Res* 2006; **83**: 392–402.
51 Song S-K, Yoshino J, Le TQ, Lin S-J, Sun S-W, Cross AH *et al.* Demyelination increases radial diffusivity in corpus callosum of mouse brain. *NeuroImage* 2005; **26**: 132–140.
52 Andersson JLR, Jenkinson M, Smith S. Non-linear registration aka spatial normalisation. FMRIB Analysis Group of the University of Oxford: Oxford, UK, 2007. FMRIB technical report TR07JA2.
53 Smith SM, Nichols TE. Threshold-free cluster enhancement: addressing problems of smoothing, threshold dependence and localisation in cluster inference. *Neuroimage* 2009; **44**: 83–98.
54 Paxinos G, Watson C. *The Rat Brain in Stereotaxic Coordinates*. Academic Press: New York, NY, USA, 1998.
55 Goldman-Rakic PS. Architecture of the prefrontal cortex and the central executive. *Ann N Y Acad Sci* 1995; **769**: 71–83.
56 Cerqueira JJ, Pêgo J, Taipa R, Bessa JM, Almeida OFX, Sousa N. Morphological correlates of corticosteroid-induced changes in prefrontal cortex-dependent behaviors. *J Neurosci* 2005; **25**: 7792–7800.

57 Jay TM, Rocher C, Hotte M, Naudon L, Gurden H, Spedding M. Plasticity at hippocampal to prefrontal cortex synapses is impaired by loss of dopamine and stress: importance for psychiatric diseases. *Neurotox Res* 2004; **6**: 233–244.
58 Brunjes PC, Illig KR, Meyer EA. A field guide to the anterior olfactory nucleus (cortex). *Brain Res Brain Res Rev* 2005; **50**: 305–335.
59 Blumenfeld-Katzir T, Pasternak O, Dagan M, Assaf Y. Diffusion MRI of structural brain plasticity induced by a learning and memory task. *PLoS One* 2011; **6**: e20678.
60 Ding AY, Li Q, Zhou IY, Ma SJ, Tong G, McAlonan GM *et al.* MR diffusion tensor imaging detects rapid microstructural changes in amygdala and hippocampus following fear conditioning in mice. *PLoS One* 2013; **8**: e51704.
61 Sagi Y, Tavor I, Hofstetter S, Tzur-Moryosef S, Blumenfeld-Katzir T, Assaf Y. Learning in the fast lane: new insights into neuroplasticity. *Neuron* 2012; **73**: 1195–1203.
62 Zatorre RJ, Fields RD, Johansen-Berg H. Plasticity in gray and white: neuroimaging changes in brain structure during learning. *Nat Neurosci* 2012; **15**: 528–536.
63 Lerch JP, Yiu AP, Martinez-Canabal A, Pekar T, Bohbot VD, Frankland PW *et al.* Maze training in mice induces MRI-detectable brain shape changes specific to the type of learning. *NeuroImage* 2011; **54**: 2086–2095.
64 Sampaio-Baptista C, Khrapitchev AA, Foxley S, Schlagheck T, Scholz J, Jbabdi S *et al.* Motor skill learning induces changes in white matter microstructure and myelination. *J Neurosci* 2013; **33**: 19499–19503.
65 Hofstetter S, Tavor I, Tzur Moryosef S, Assaf Y. Short-term learning induces white matter plasticity in the fornix. *J Neurosci* 2013; **33**: 12844–12850.
66 Assaf Y, Pasternak O. Diffusion tensor imaging (DTI)-based white matter mapping in brain research: a review. *J Mol Neurosci* 2008; **34**: 51–61.
67 Markham JA, Greenough WT. Experience-driven brain plasticity: beyond the synapse. *Neuron Glia Biol* 2004; **1**: 351–363.
68 Sanchez I, Hassinger L, Paskevich PA, Shine HD, Nixon RA. Oligodendroglia regulate the regional expansion of axon caliber and local accumulation of neurofilaments during development independently of myelin formation. *J Neurosci* 1996; **16**: 5095–5105.
69 Klawiter EC, Schmidt RE, Trinkaus K, Liang HF, Budde MD, Naismith RT *et al.* Radial diffusivity predicts demyelination in *ex vivo* multiple sclerosis spinal cords. *NeuroImage* 2011; **55**: 1454–1460.
70 Sun SW, Liang HF, Le TQ, Armstrong RC, Cross AH, Song SK. Differential sensitivity of *in vivo* and *ex vivo* diffusion tensor imaging to evolving optic nerve injury in mice with retinal ischemia. *NeuroImage* 2006; **32**: 1195–1204.
71 Scholz J, Klein MC, Behrens TEJ, Johansen-Berg H. Training induces changes in white-matter architecture. *Nat Neurosci* 2009; **12**: 1370–1371.